

# Cosmic Phase Transitions

B. Kämpfer<sup>1</sup>

<sup>1</sup>Forschungszentrum Rossendorf, Postfach 510119, 01314 Dresden, Germany  
kaempfer@fz-rossendorf.de

Received 28 April 2000, accepted 06 July 2000 by F.W. Hehl

**Abstract.** The sequence of phase transitions during the hot history of the universe is followed within a phenomenological framework. Particular emphasis is put on the QCD confinement transition, which is at reach under earth laboratory conditions. A tepid inflationary scenario on the GUT scale with bubble growth at moderate supercooling is discussed.

**Keywords:** cosmic phase transitions, deconfinement, inflation

**PACS:** 04.40.-b, 24.85, 98.80.Cq, 64.60.Qb

## 1 Introduction

The standard cosmology teaches that the universe is expanding. This implies a steady change of the state of matter. Particularly interesting are phase transitions where the structure and the relevant degrees of freedom change. Probably the most drastic transition was the formation of the early universe. There is a number of ideas how did this happen, including the creation from a quantum state (cf. [1] and further references there). Since the extrapolation of our quantum field theoretical models to high temperature and density points to a maximum temperature of  $T \sim 10^{16}$  GeV, where thermal equilibrium between various particles can be maintained, one can guess that the thermal history starts at such a temperature scale and corresponding world age of  $10^{-37}$  sec. Immediately afterwards one conjectures that a symmetry breaking phase transition happens. At a scale of  $T \sim 10^{16}$  GeV, or slightly less, the extrapolated coupling strengths of the strong, weak and electromagnetic interactions merge, and one generally believes that the behavior of matter is to be described within the framework of a grand unified theory (GUT). The very structure of GUT is still matter of debate, and also the relation to supersymmetric and string theories is not yet settled down. Nevertheless, inflation, i.e. a stage of accelerated expansion and a huge blowing off of the space is an important scenario, which allows to understand some of the presently observed properties of the universe.

The subsequent evolution appears quite unspectacular for a long time span: expansion means cooling, and particles with masses in the order of 40% of the corresponding temperature disappear due to annihilation.

The next interesting stage is the symmetry breaking on the electroweak scale, i.e.  $T \sim 100$  GeV. Cooling further, at  $T \sim 160$  MeV the quarks and gluons, roaming up to this stage freely, become bound in hadrons. This is the confinement transition, which might be called the hadrosynthesis stage.

Once the temperature falls below 1 MeV the nucleosynthesis starts, creating the light primordial elements. In nuclear matter, a liquid-gas phase transition is conjectured since a long time (cf. [2]), and experimental hints have been verified [3]. However, in the cosmic evolution this transition does not play a role since it is related to large baryon density.

From such a point of view the history of the early universe can be considered as sequence of phase transitions. Indeed, based on quite general models, one can develop a scheme to combine the dynamics of phase transitions with the cosmic expansion, as envisaged in [4]. Here we follow, however, a different avenue and consider the specific features of individual transitions.

Among the above mentioned phase transitions the confinement transition from quarks and gluons to hadrons has been elaborated by far in most details. This is because it is believed to be reproducible in the laboratory. Indeed, for colliding nuclei at sufficiently high energies, the relevant degrees of freedom should be represented by partons, i.e. point-like structures. The presently terminating first round of heavy-ion experiments at CERN accumulated such a wealth of data which give rise to the interpretation that in central nuclear collisions a thermalized state of delimitated quarks and gluons has been created. Indeed, on February 9, 2000 a press release of CERN announced “compelling evidence for the existence of a new state of matter in which quarks, instead of being bound up into more complex particles such as protons and neutrons, are liberated to roam freely, ... this state must have existed at about 10 microseconds after the Big Bang” [5].

In accordance with this new information we will focus here on the confinement transition after the Big Bang. We will compare schematically the confinement dynamics of the Big Bang with that of the Little Bang (i.e. relativistic heavy-ion collisions). By using the known details of the transition we demonstrate the interplay of local matter properties and global evolution dynamics. More specifically, we analyze how drives the local matter state the global expansion, and vice versa, how the expansion causes cooling and transformation of matter forms into each other.

There is some apparent similarity in cosmology and heavy-ion physics, which we try to visualize in Fig. 1. From present observations of remote objects in the universe, we look somewhat into the past. Combining observational facts, like the distribution and the red shift of galaxies, as seen in the left panel of Fig. 1, one can develop a picture of the early stages of the universe. The situation in heavy-ion physics is very similar to this. Observing the created hadrons in a very late stage, one tries to extrapolate back to the hottest and densest stages. The artist’s view of a semi-peripheral collision of heavy-ions, displayed in the right panel of Fig. 1, shows a stage where the matter is converted into hadrons which still interact for a while before disassembling. However, there is a chance in heavy-ion collisions to receive a direct signal of the very early stage: the mean free path of real and virtual photons [7] is large in comparison with the system size. For such direct probes the problem, however, arises to disentangle the primordial signal from a huge background [8].

The present survey is restricted to a phenomenological framework. That means, we do not go into a microscopic theory of phase transitions, rather describing them only in terms of the equation of state. We restrict ourselves to the standard model and the grand unifying theory models of the strong and electroweak interactions. Only

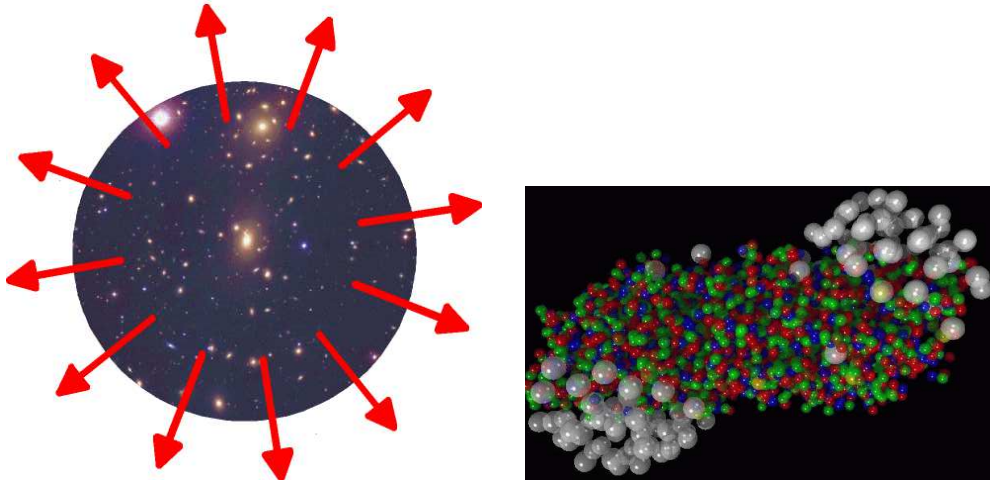


**Fig. 1** Expanding matter: The left panel displays a view on a group of remote galaxies as seen by the Hubble telescope (source of the underlying picture: NASA picture gallery in [www](#) [6]), while the right panel shows the distribution of hadrons in a semi-peripheral collision of heavy nuclei a few fm/c after the first touch (source: CERN press release in [www](#) [5]).

in a few exceptional cases we quote interesting effects occurring beyond the standard model of particle physics within supersymmetric or string-theoretical models.

The paper is organized as follows. In section 2 the phenomenological framework is presented resulting in Friedmann's equations for the Big Bang and the corresponding equations of matter in the Little Bang. Section 3 deals with quantum chromodynamics (QCD), quarks and gluons and their equation of state. Section 4 exercises a simple way to construct first-order phase transitions. The basic issues of nucleation theory for handling the phase transformation dynamics are presented in section 5. Section 6 is devoted to details of the cosmic confinement transition. A short remark concerning the present status of knowledge on the electroweak transition is made in section 7. In section 8 we deal with an attempt of a phenomenological realization of an inflationary scenario. The summary can be found in section 9.

The material represented is based on [www](#) scans till end of April 2000.

## 2 Phenomenological framework

Our phenomenological considerations are based on two cornerstones, namely the description of

- (i) local matter properties within the framework of thermodynamics and hydrodynamics, and
- (ii) global cosmic expansion by Einstein's equation and the cosmological principle.

We are now going to present these issues and define the propositions.

## 2.1 Einstein equations

The Einstein equations can be written as

$$R_{ij} - \frac{1}{2}g_{ij}\hat{R} = \kappa\hat{T}_{ij}, \quad \kappa = \frac{8\pi G_N}{c^4}, \quad (1)$$

which can be interpreted as gravity, described by geometry or curvature of the space-time on the left-hand-side, being caused by matter, which in turn is described by the phenomenological energy momentum tensor,  $\hat{T}_{ij}$ , on the right-hand-side. More specifically,  $R_{ij}$  is the Ricci tensor,  $\hat{R} = R_{ij}g^{ij}$  the curvature scalar, and  $g_{ij}$  the metric. The Newtonian constant  $G_N$  serves as coupling strength of geometry to its source, i.e. to matter. In the following we employ mainly units from particle physics, i.e.  $\hbar = c = k_B = 1$  for the Planck quantum divided by  $2\pi$ , and velocity of light, and Boltzmann's constant, respectively.<sup>a</sup> The energy-momentum tensor can be split into a vacuum part,  $T_{ij}^{\text{vac}}$ , and a matter part,  $T_{ij}$ , accounting for excitations above the vacuum:

$$\hat{T}_{ij} = T_{ij}^{\text{vac}} + T_{ij}, \quad T_{ij}^{\text{vac}} = (e^{\text{vac}} + p^{\text{vac}})u_i u_j - p^{\text{vac}}g_{ij}, \quad (2)$$

where  $e^{\text{vac}} = -p^{\text{vac}}$  ensures the local Lorentz invariance of the vacuum. The presently observed accelerated expansion of the universe [9] could be caused a dominating vacuum energy  $e^{\text{vac}} \approx 5 \times 10^{-30} \text{g} \cdot \text{cm}^{-3} \approx 0.6 e^{\text{crit}} \approx 10^{-123} M_{\text{Pl}}^4$  [10]. Here,  $M_{\text{Pl}} = 1.22 \times 10^{19} \text{GeV} = 2.17 \times 10^{-5} \text{g}$  stands for the Planck mass defined by  $M_{\text{Pl}} = \sqrt{\hbar c / G_N}$ . The vacuum energy is the missing link to add up all energy forms, including the substantial part of dark matter [11], to an amount corresponding to a flat universe with  $e = e^{\text{crit}}$ , which is "predicted" by inflationary scenarios. The present critical energy density is  $h^2 1.88 \times 10^{-29} \text{g cm}^{-3}$  with  $h \approx 0.68$  [12].

From the Friedmann equations (see (16) below) a less negative "vacuum" pressure of  $p^{\text{vac}} \leq -\frac{1}{3}e^{\text{vac}}$  is enough to drive an accelerated expansion. The present vacuum energy could be generated by evolving fields, e.g. the tracker fields [13]. This would cause a noticeable uncertainty in extrapolating back to the early history of the universe, because the relation of the vacuum energy density to the energy density of other matter forms is rather unsettled.

If the vacuum energy, sometimes also dubbed quintessence [14], would be constant, then it can comfortably be included in Einstein's famous cosmological constant  $\Lambda = e^{\text{vac}}\kappa = \text{const}$ , and the Einstein equations would read

$$R_{ij} - \frac{1}{2}g_{ij}\hat{R} - \Lambda g_{ij} = \kappa T_{ij}. \quad (3)$$

In such a case, the vacuum energy can be neglected at early times, i.e.  $e^{\text{vac}} \ll e$ . We do not touch upon the questions on the origin of the cosmological constant [15] or why the vacuum energy is becoming operative just now, but we assume in the following that the present vacuum energy can be neglected at early times in comparison with other energy contributions. We mention in advance that in certain cosmic stages appropriate vacua are included.

<sup>a</sup> The conversion constant  $\hbar c = 197.327053 \text{ MeV} \cdot \text{fm}$  is useful for relating length scales and energy scales and for translations into other unit systems as well.

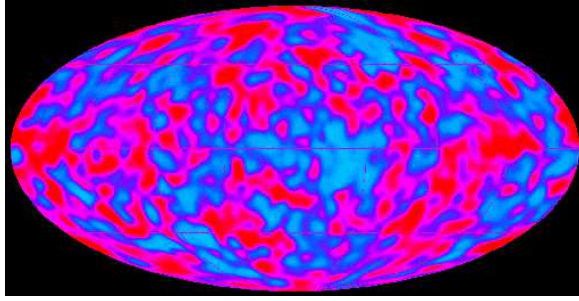


**Fig. 2** A contour plot of the temperature distribution in the universe at last rescattering of photons as seen by the cosmic background explorer satellite COBE (source: NASA picture gallery in [www](#) [17]).

## 2.2 Cosmological principle and Robertson-Walker metric

The cosmological principle requires homogeneity and isotropy resulting in a simple space-time symmetry according to  $SO(4)$ , or  $E(3)$ , or  $SO(3,1)$  symmetry groups<sup>b</sup> and the Robertson-Walker metric (e.g. cf. [16])

$$ds^2 = dt^2 - R(t)^2 \left( \frac{dr^2}{1 - kr^2} + r^2 d\Omega^2 \right), \quad (4)$$

where the only dynamical quantity is the scale factor  $R(t)$ . The parameter  $k = \pm 1, 0$  determines whether the universe has a closed, open, or flat geometry. For early cosmology and our purposes it is sufficient to consider the case  $k = 0$ .

The present microwave background radiation corresponds to a blackbody radiation with temperature of  $T = 2.7277$  K with relative fluctuations less than  $10^{-4}$ . The cosmic background explorer COBE quantifies these fluctuations, as shown in Fig. 2. This COBE map may be understood as a snapshot of the universe at the age of 400,000 years. While the tiny fluctuations have been amplified during the last 14 Gigayears to the present structures, like galaxies and clusters, the very early stages of the universe can be assumed to be very smooth.

## 2.3 Perfect fluid

In the following we describe matter by the energy-momentum tensor

$$T_{ij} = eu_i u_j + q_i u_j + u_i q_j + p_{ij}, \quad (5)$$

where  $e$  is the energy density. The stress part,  $p_{ij}$ , is orthogonal to the four-velocity  $u_i$  of matter, i.e.  $p_{ij}u^i = 0$ , as is the energy flow  $q_i$ . Within this framework, matter is described by a fluid thus covering special cases as dust, real fluid, gas, and vacuum. In (5) it is assumed that one unique velocity field is common to all subcomponents

<sup>b</sup> We do not consider the Kantowski class which has no local Minkowski limit.

of matter. There are two possible gauges of the velocity: either according to Landau, with  $u_i$  parallel to energy flow, or according to Eckart, with  $u_i$  parallel to baryon flow. Since we neglect in most examples the baryon charge, the Eckart gauge is applied.

In the following we mainly consider non-dissipative media, i.e. heat conductivity and shear viscosity and possible other gradient terms with non-standard dissipative effects [18] are not included. The only dissipative effect we consider in subsection 8.1 is the volume viscosity parameterized by the coefficient  $\hat{\xi}$  entering the stress via

$$p_{ij} = (p - \hat{\xi} u^i{}_{;i})(-g_{ij} + u_i u_j), \quad u^i u_i = +1. \quad (6)$$

The entropy current then reads

$$s_i = s u_i \quad (7)$$

and has to satisfy  $s^i{}_{;i} \geq 0$ ; here  $s$  is the entropy density; the semicolon, “;”, denotes the covariant derivative. (5, 6) with  $\hat{\xi} = 0$  define the perfect fluid.

#### 2.4 Equations of motion of perfect fluid in Big Bang

Discarding any dissipative effect we now present the equations of motion of matter and geometry for the Big Bang. Since the cosmic matter consists of several components, labeled by  $\alpha$ , we take into account

$$e = \sum_{\alpha} e_{\alpha}, \quad p = \sum_{\alpha} p_{\alpha}. \quad (8)$$

##### 2.4.1 Robertson-Walker metric

The four velocity in comoving coordinates is  $u_i = \delta_i^0$  yielding with the metric (4)

$$u^i{}_{;i} = 3 \frac{\dot{R}}{R}. \quad (9)$$

##### 2.4.2 Projection of the contracted Bianchi identity

The projection of the contracted Bianchi identity  $u_i T^{ij}{}_{;j} = 0$  yields

$$\dot{e} + 3 \frac{\dot{R}}{R}(e + p) = 0 \quad (10)$$

for the perfect fluid.

##### 2.4.3 Current conservation

If there are  $\beta$  conserved currents,  $(n_{\beta} u^i)_{;i} = 0$ , the conservation of the corresponding charges reads

$$\dot{n}_{\beta} + 3 \frac{\dot{R}}{R} n_{\beta} = 0 \quad \rightarrow \quad n_{\beta} R^3 = const. \quad (11)$$

The quantities  $n_{\beta}$  can represent the baryon density, or the electric charge density etc.

#### 2.4.4 Einstein's equations

For  $\Lambda = 0$  the Einstein equations (1) read

$$R_{ij} - \frac{1}{2}g_{ij}\hat{R} = 3\mathcal{C}^2\hat{T}_{ij}, \quad \mathcal{C} \equiv M_{\text{Pl}}^{-1}\sqrt{\frac{8\pi}{3}}. \quad (12)$$

A consideration of  $T_{11} - \hat{R}T_{00}$  and the corresponding left hand side of (12) yields

$$\dot{R} = \sqrt{\mathcal{C}^2 R^2 e - k}. \quad (13)$$

For  $k = 0$  these equations can be combined to result in

$$\dot{R} = \mathcal{C}R\sqrt{e}, \quad (14)$$

$$\dot{e} = -3\mathcal{C}(e+p)\sqrt{e}. \quad (15)$$

(Notice that for early cosmology the distinction of  $k = \pm 1$  or 0 is usually not important.) To integrate the latter equation, an equation of state,  $p(e)$ , is needed. It should be emphasized that the derivation above does not invoke entropy conservation.

The  $i = 0, j = 0$  component of the Einstein equations (12) reads

$$\ddot{R} = -\frac{1}{2}\mathcal{C}^2 R(e+3p). \quad (16)$$

This shows that  $e+3p > 0$  results in  $\ddot{R} < 0$ , i.e., a decelerated expansion, while  $e+3p < 0$  means  $\ddot{R} > 0$ , i.e., an accelerated expansion.

#### 2.5 Equations of motion for the Little Bang

Various dynamical models [19] suggest that in a very high-energetic collision of nuclei the initial conditions on proper time hypersurfaces (see left panel of Fig. 3)  $\tau = \sqrt{t^2 - z^2} = \text{const}$  are constant. In suitable coordinates, namely the proper time  $\tau$  and the rapidity  $Y = \text{atanh}(z/t)$ , this looks like a homogeneously longitudinally expanding fire cylinder (see right panel of Fig. 3). We neglect the onset of transversal expansion, i.e.,  $v_x = v_y = 0$ . Then the motion is called scale invariant or boost invariant expansion [20], which is described by the four-velocity  $u^i = \gamma(1, 0, 0, v_z)$  with  $v_z = z/t$  and  $\gamma = (1 - v_z^2)^{-1/2}$ .

The corresponding equations of motion for the perfect fluid then read

$$\dot{e} = -\frac{1}{\tau}(e+p) \quad (17)$$

from  $u_i T^{ij}_{;j} = 0$  (a dot means here derivative with respect to  $\tau$ ), and

$$n_\beta \tau = \text{const} \quad (18)$$

from  $(n_\beta u^i)_{;i} = 0$ . To integrate (17) again the equation of state  $p(e)$  is needed.

Employing a simple equation of state like  $p = aT^4$  with  $a \sim \mathcal{O}(1)$  and the thermodynamic relations from the next subsection, the dynamical time scales in Little Bang and Big Bang can be estimated as

$$\text{Little Bang: } \frac{e+p}{e} \sim \tau \sim \tau_1 \sim 1 \text{ fm/c} \quad (19)$$

$$\text{Big Bang: } \frac{e+p}{\dot{e}} \sim \frac{M_{\text{Pl}}}{\sqrt{e}} \sim 10^{19} \text{ fm/c}, \quad (20)$$

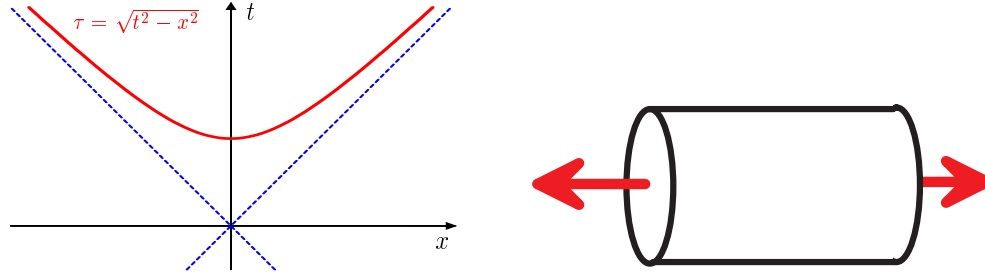


**Fig. 3** Symmetry of a high-energy heavy-ion collision. Left panel: Incoming nuclei move nearly on the light cone (dashed lines); the thermalized matter has constant energy density and baryon density on the hyperboloid of constant proper time  $\tau$ . Right panel: Before the onset of transverse expansion the matter expands homogeneously in longitudinal direction.

where  $1 \text{ fm}/c = 3 \times 10^{-24} \text{ sec}$ , and we used a temperature scale of  $T \sim 0.2 \text{ GeV} \sim 2 \times 10^{12} \text{ K}$ . Eq. (20) shows that (i) higher energy densities cause faster expansion, and (ii) the time scale of the Big Bang is determined by the Planck mass.

## 2.6 Thermodynamics

To complete the list of propositions let us recall the thermodynamic relations for a single-component and single-phase medium:

$$\text{thermodynamic potential: } p(T, \mu), \quad (21)$$

$$\text{Gibbs relation: } e + p - Ts = \mu n, \quad (22)$$

$$\text{Euler relations: } s = \frac{\partial p}{\partial T}, \quad n = \frac{\partial p}{\partial \mu}, \quad (23)$$

where  $\mu$  is the chemical potential and  $n$  the related conserved charge density.

For the early universe, one estimates from present observations and from Big Bang nucleosynthesis calculations,  $\frac{n_B}{n_\gamma}|_{t_*} \sim 10^{-10}$  (here  $n_B$  is the baryon density and  $n_\gamma$  the photon density), via entropy conservation a baryo-chemical potential  $\frac{\mu_B}{T} \sim 10^{-9}$ . Therefore, for many purposes one can neglect effects of a finite baryon charge, unless one is dealing with the evolution of the baryon density itself. The estimates for the lepto-chemical potentials are not on such firm grounds due to the non-observability of the neutrino background; but one usually assumes similarly small lepto-chemical potentials.

From the quantum statistics of ideal gases one finds the pressure as a thermodynamic potential

$$p = \sum_s \pm \frac{d_s}{2\pi^2} T^4 \int_0^\infty dx x^2 \ln \left[ 1 \pm \exp \left\{ \frac{\mu_s}{T} - \sqrt{\left( \frac{m_s}{T} \right)^2 + x^2} \right\} \right] \quad (24)$$

$$\approx \sum_{m_s \ll T} d_s \frac{\pi^2}{90} T^4 = aT^4, \quad (25)$$

Little Bang:

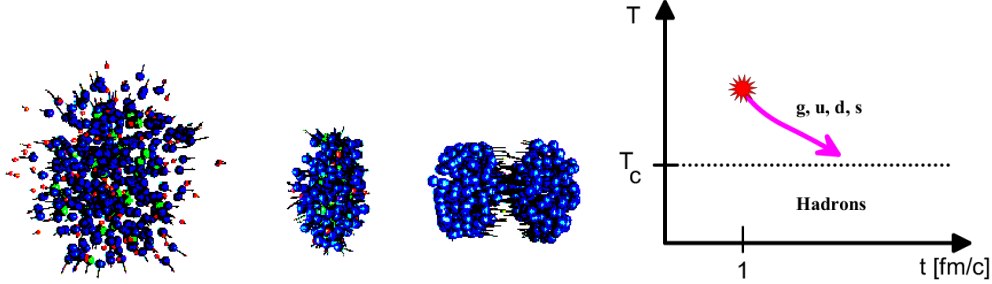


**Fig. 4** Left three panels: An artist's view on a central heavy-ion collision (right: the approach stage before first touch, middle: highly compressed strongly interacting matter is formed; in the center of the blob quarks and gluons are the relevant degrees of freedom, left: the system has completely transformed to hadrons and expands. Pictures by S. Bass exploiting a transport model). Right panel: A sketch of the temperature evolution till confinement.

where  $s$  labels the particle species,  $d_s$  their effective degeneracies (being the number of degrees of freedom for each boson, and  $\frac{7}{8} \times$  the number of degrees of freedom for each fermion, respectively); the upper (lower) sign in (24) is for fermions (bosons). The pressure is dominated by those particle species with masses  $m_s$  lower than the temperature  $T$ . This toy model equation of state gives the time evolution of the temperature and entropy density

$$\text{Little Bang: } T = T_1 \left(\frac{\tau_1}{\tau}\right)^{1/3}, \quad s\tau = \text{const}, \quad (26)$$

$$\text{Big Bang: } T = (2\sqrt{3}aCt)^{-1/2}, \quad sR^3 = \text{const}, \quad (27)$$

where  $T_1$  is the maximum temperature at which the system is thermalized and  $\tau_1$  the corresponding time. Clearly, the comoving entropies are constant.

### 2.7 Little Bang vs. Big Bang

One can visualize the similarities and differences of the evolution of matter in the Little Bang and the Big Bang as follows. Let us consider in both cases high enough temperatures, so that the strongly interacting matter component is in a deconfined state. Initially, in the Little Bang (see Fig. 4) the nuclear matter is in its ground state. The uni-directional motion during the approach stage has zero entropy. During the virulent collision this motion is randomized and a substantial part of the kinetic beam energy is converted into particle excitations. According to dynamical models [19], after a time scale of  $\tau_1 \sim \mathcal{O}(1 \text{ fm}/c)$  or even shorter, the matter is locally equilibrated and may be characterized by an initial or maximum temperature  $T_1$ .

According to present estimates the maximum temperatures are  $\mathcal{O}(200)$  MeV for CERN-SPS<sup>c</sup> [21],  $\mathcal{O}(550)$  MeV for BNL-RHIC<sup>d</sup> and  $\mathcal{O}(1000)$  MeV for CERN-LHC<sup>e</sup>

<sup>c</sup> Super Proton Synchrotron at CERN, i.e. the European Laboratory for Particle Physics in Geneva

<sup>d</sup> Relativistic Heavy-Ion Collider at Brookhaven National Laboratory

<sup>e</sup> Large Hadron Collider at CERN

Big Bang:

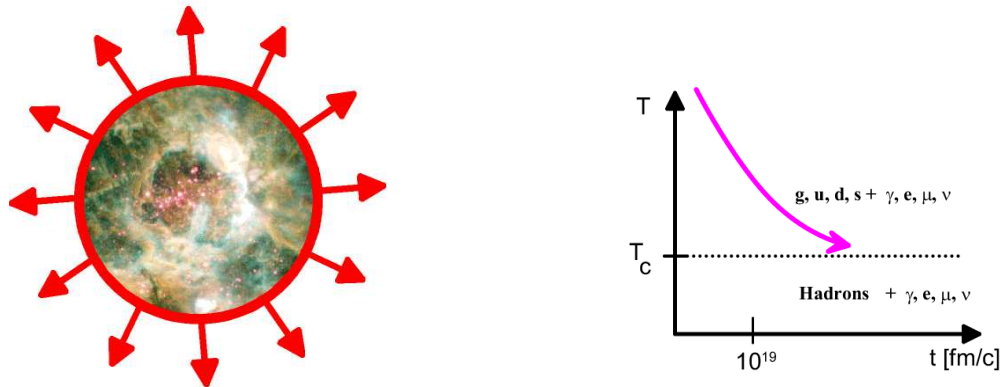


**Fig. 5** Left panel: A sketch of the expanding universe. Right panel: A sketch of the temperature evolution till confinement.

[22]. As mentioned above, already at CERN-SPS energies the body of observational material is in agreement with the expectation of having produced a state of strongly interacting matter where gluons and quarks are the relevant degrees of freedom, abbreviated in the very right panel in Fig. 4 by  $g, u, d, s$ . Due to the enormous pressure the system expands and converts into hadrons, eventually registered in detectors. Note that, despite of the many measured particle species, including the direct probes [7, 8, 21], a simple “yes” or “no” signal, whether a deconfined state is transiently created in heavy-ion collisions, is not at disposal. Instead, rather a combination of various, partially subtle, observables allows the conclusion to have produced a quark-gluon plasma. In contrast to the situation in the cosmic evolution, under laboratory conditions the beam energy can be changed, and within some limits the system size can be varied as also the impact parameter.

Presumably, the evolution of matter in the Big Bang (see Fig. 5) started at much higher temperature. Note again the difference of the time scales in Figs. 4 and 5. In addition, in the Big Bang there is the non-negligible contribution of the photon and lepton background, as indicated in Fig. 5, which is in kinetic and chemical equilibrium with the strongly interacting matter.

There is a simple argument that dense strongly interacting matter must change its state. Consider a hadron system at temperature of  $T \sim 100$  MeV. There are mostly pions excited with an admixture of kaons, etas, omega and rho mesons, and a few nucleons and their anti-particles. At higher temperature, say around  $T \sim 150$  MeV the hadrons start touching each other since they have a finite spatial extension on the scale of 1 fm (see Fig. 6). At slightly higher temperatures, the hadrons cannot be longer the proper degrees of freedom. Instead the matter consists of quarks and gluons. Probably also the vacuum structure changes, as indicated by a different gray scale in the background of the right panel of Fig. 6.

Now, we are now interested in the dynamics of the confinement transition, i.e., the conversion of deconfined quarks and gluons into hadrons.

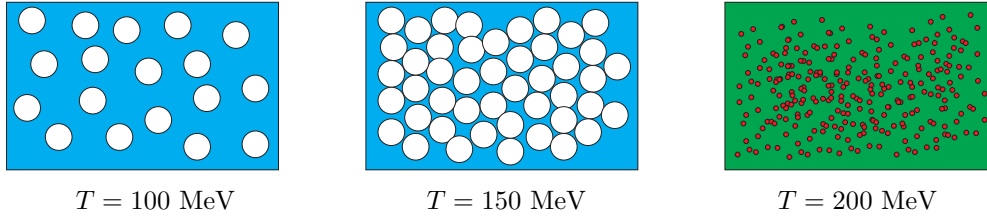


**Fig. 6** A sketch of strongly interacting matter at various temperatures. Left and middle panels: Hadrons with finite extension are the relevant degrees of freedom. Right panel: Point-like quarks and gluons are the relevant degrees of freedom, the vacuum state is changed.

### 3 QCD, quarks & gluons, confinement

In order to describe the transition from quark-gluon matter to hadron matter in more detail one has to rely on the proper theory of strong interaction, i.e. QCD. It rests on the Lagrange density (cf. [23] for details, e.g.)

$$\mathcal{L} = \bar{\psi}(i\gamma_j D^j - \mathcal{M})\psi - \frac{1}{4}F_{ij}^a F^{ij}_a \quad (28)$$

with exact local SU(3) gauge symmetry.  $D^j$  is the gauge covariant derivative,  $\psi$  and  $\bar{\psi}$  stand for Dirac spinors and their adjoints,  $\gamma_j$  are Dirac's matrices, and  $F_{ij}^a$  denotes the field strength tensor of the non-Abelian gauge fields. Since the different quark flavors have different masses,  $\mathcal{M}$  in (28) denotes the mass matrix.

Renormalization on the one-loop level results in the running strong coupling strength

$$\alpha_s(Q^2) = \frac{4\pi}{\beta_0 \ln\left(\frac{Q^2}{\Lambda_{\text{QCD}}^2}\right)}, \quad \beta_0 = 11 - \frac{2}{3}N_f \quad (29)$$

via dimensional transmutation with the QCD scale  $\Lambda_{\text{QCD}} \sim \mathcal{O}(200) \text{ MeV}$ ;  $N_f$  is the number of involved quark flavors. In a system with a very large momentum scale  $Q^2$ , the asymptotic freedom follows immediately from (29), i.e.,  $\lim_{Q^2 \rightarrow \infty} \alpha_s \rightarrow 0$ . Indeed, if in a gas of quarks and gluons the momentum scale increases with increasing temperature, one expects asymptotically an ideal gas. In contrast, at  $T \rightarrow T_c$ , the system is strongly coupled and perturbative calculations basically fail.

The only reliable way of *ab initio* calculations of thermodynamical properties of a quark-gluon plasma is to perform Monte Carlo simulations of finite temperature QCD in a discretized space-time. A few results of such lattice QCD calculations are displayed in Fig. 7 together with results of a quasi-particle model [24] with parameters adjusted to the data.

The transition temperature is estimated as  $T_c \sim 160 \text{ MeV} \sim \mathcal{O}(m_\pi) \sim 1.6 \times 10^{12} \text{ K}$  for a quark-gluon plasma, while for a pure gluon gas it would be  $T_c^{\text{glue}} \sim 240 \text{ MeV}$  ( $m_\pi$  is the pion mass). Note that the present lattice QCD calculations cover only the region  $T > T_c$  and  $\mu = 0$ . In order to describe the equation of state for hadron matter below  $T_c$  reliably, a prerequisite would be an accurate description of the mass spectrum of the hadrons, a goal not yet fully accomplished. Despite the lack of an equation of state at  $T < T_c$ , some information on the order of the transition is available. Inspection

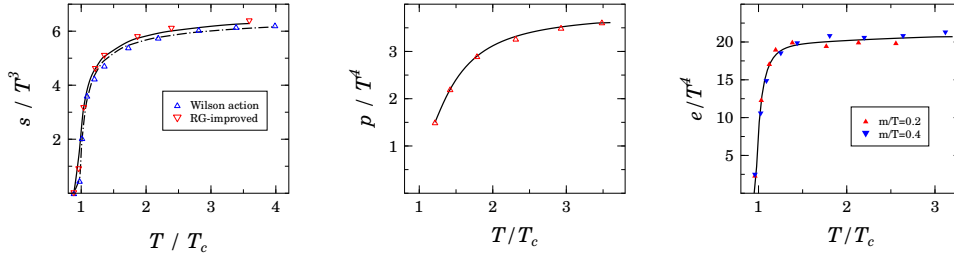


**Fig. 7** Thermodynamics of a gluon gas (left panel) and a two-flavor (middle panel) and a four-flavor (right panel) quark-gluon plasma as a function of the scaled temperature. Lattice QCD results (symbols) from the Bielefeld group. The curves represent an adjusted quasi-particle model, for details consult [24].

of the left panel of Fig. 8 reveals that if the masses of the light current quarks are sufficiently small the deconfinement transition is of first order. The physical relevant case of the two light flavors  $u, d$  and a medium-heavy  $s$  quark is near to the borderline to a cross over. The latter notion means a dramatic, but nevertheless smooth change of thermodynamic properties in a narrow region around  $T_c$ . At sufficiently small  $u, d$  quark masses and large  $s$  quark mass, the phase transition would be of second order; the regions of first order and second order are separated by a tri-critical point. The pure gauge sector (i.e., infinitely heavy quarks so that they do not longer act as dynamical objects) is known to display a first-order phase transition again.

Since in the early universe the baryo-chemical potential is small the information on the region  $\mu > 0$  is not important. Otherwise, in the Little Bang (or more importantly, in massive neutron stars with quark cores) the finite baryo-chemical potential  $\mu$  becomes important. As seen in the right panel of Fig. 8, a richer structure of the phase diagram is showing up with di-quark condensates (2SC) and color-flavor locking effects (CFL); also an endpoint (E) of the phase borderline may appear at finite values of  $T$  and  $\mu$  (for more details, see [26]). The latter peculiarities make the previous naive phase diagram, as shown in Fig. 9, more involved.

To quote some physical numbers characterizing the nuclear matter near ground state one can refer to  $n_0 = 0.15 \text{ fm}^{-3} = 1.5 \times 10^{38} \text{ cm}^{-3}$ ,  $e_0 = 2.7 \times 10^{14} \text{ g cm}^{-3}$ ,  $1 \text{ MeV} \approx 10^{10} \text{ K}$ .

The deconfinement transition is intimately related to chiral symmetry restoration at temperature  $T_c^\chi$ . In hadronic matter, at  $T < T_c^\chi$ , the effective degrees of freedom are massive quarks and we have finite expectation values of condensates, like the chiral condensate  $\langle \bar{\psi}\psi \rangle$ . For  $T > T_c^\chi$  the quarks become massless and the condensates disappear. For QCD it turns out that deconfinement and chiral symmetry restoration coincide, i.e.  $T_c = T_c^\chi$ . Therefore, the chiral condensate may serve as order parameter describing the confinement.

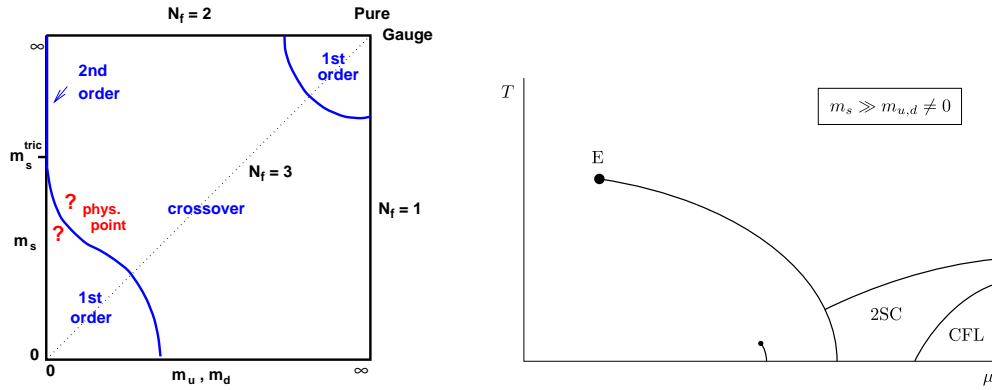


**Fig. 8** Phase diagrams of strongly interacting matter. Left panel: The order of the phase transition as a function of the quark mass parameters (from [25]). Right panel: The phase diagram in the  $T - \mu$  plane according to [26].

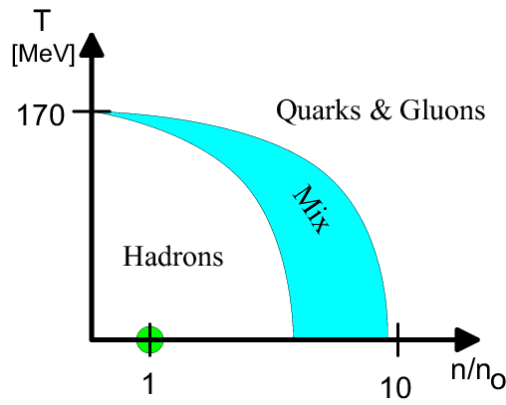


**Fig. 9** Naive phase diagram of strongly interacting matter in the  $T - n$  plane ( $n$  is the baryon density).

#### 4 A constructed phase transition of first order

In view of the above discussion of the order of the deconfinement transition, it seems legitimate to approximate the thermodynamics in the transition region by a suitable construction. This construction results in a strong first-order phase transition with large latent heat (cf. Fig 11) which probably overestimates of what we can expect in reality. The construction, however, is made quite general so that it might be applied also in other cosmic phase transitions, such as on electroweak and GUT scales to be discussed below. A MIT-type bag model is quite popular: asymptotically free quarks are confined in a certain spatial region, called bag. The vacuum energy density in the bag is enlarged by a constant amount of  $B$  when compared with ordinary vacuum. The equation of state reads then

$$p_{\text{QCD}} = d_{g,u,d} \frac{\pi^2}{90} T^4 - B, \quad d_{g,u,d} = 37, \quad (30)$$

with vacuum pressure  $-B$ . The use of the pure radiation term  $\propto T^4$  is suggested by asymptotic freedom; near to  $T_c$ , the non-perturbative effects are thought to be parameterized by  $B$ . This ansatz allows only a poor reproduction of the lattice QCD results, and for more detailed considerations it must be replaced by other models like that in [24]. In some sense this schematic equation of state can be considered as a down-extrapolation from asymptotic freedom. Similarly, one can up-extrapolate the hadron equation of state, and the most simple ansatz is that of a pion gas neglecting the strong interaction:

$$p_\pi = d_\pi \frac{\pi^2}{90} T^4, \quad d_\pi = 3. \quad (31)$$

Also this too simple model needs improvements by including the other hadrons (cf. [27]) and their strong interactions. In [28] the interested reader can find a selection of some recent approaches and various methods. Despite of many efforts, a generally accepted nuclear or hadronic equation of state at large temperature and density has not yet emerged. A direct comparison of the various model equations of state with experimental data from heavy-ion collisions at BEVALAC, SIS and AGS energies (i.e., beam energies of  $1 \cdots 2$  and  $10 \cdots 15$  A-GeV) is hampered by dynamical and non-equilibrium effects [29]. A recent survey can be found in [30].

The equations of state (30, 31) are displayed in Fig. 10. At the crossing of both curves, the Gibbs conditions of phase equilibrium are fulfilled, i.e.,

$$p_1 = p_2, \quad (32)$$

$$T_1 = T_2, \quad (33)$$

$$\mu_1^{(1)} = \mu_2^{(1)}, \quad (34)$$

$$\mu_1^{(2)} = \mu_2^{(2)}, \quad (35)$$

...

Here we consider the special case of  $\mu^{(\alpha)} = 0$ . In the case of competing phases, the stable one is that with lower free energy, which is the negative of pressure. The dashed

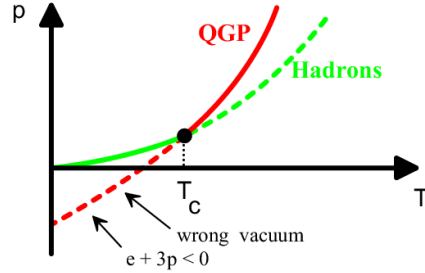


**Fig. 10** A constructed phase transition of first order by extrapolating asymptotic equations of states. The dashed branches are metastable.

sections in Fig. 10 are, therefore, metastable branches. According to the Gibbs criteria, the conditions for phase equilibrium are fulfilled at  $T_c = \frac{90}{34\pi^2} B^{1/4}$ .

Fig. 11 sketches the other thermodynamical state variables as a function of the temperature and the energy density.

Having the two asymptotic branches (30, 31) at hand, one can find, of course, also smooth interpolations between them [31] displaying a crossover. Or, as exercised in [32], one can construct another interpolation with a loop structure in the potential  $p(T)$ ; this yields two metastable and one unstable branches, as known from the famous Maxwell or double-tangent constructions. Thereby the strong phase transition of first order constructed above becomes weaker. However, the mentioned procedures are *ad hoc* and need to be checked carefully against the results of lattice QCD calculations.

## 5 Phase transformation dynamics

In spite of the simplified nature of the phase transition constructed in the previous section, we study its implications for the cosmic evolution. As stressed above, this construction overestimates the strength of the transition. Therefore, this model serves as an upper bound of possible interesting effects caused by the confinement transition.

Our discussion is based on the classical nucleation theory, where the central quantity is the critical bubble of the newly forming phase. The change of the Helmholtz free energy can be expanded into a power series with respect to the bubble radius  $r$  as

$$\Delta F(r, T) = -\frac{4\pi}{3} \Delta p r^3 + 4\pi\sigma r^2 - 8\pi\gamma r + \dots \quad (36)$$

with  $\Delta p = p_1 - p_2$  as pressure difference of both phases,  $\sigma$  is the surface tension, and  $\gamma$  the curvature parameter. Neglecting the latter one, the resulting critical radius, related to the maximum of the free Helmholtz energy, is  $R_c = \frac{2\sigma}{p_1 - p_2}$ ; smaller bubbles are energetically unfavorable since the surface energy is too large in comparison with the volume energy, while larger bubbles are too rare to influence the phase transformation dynamics. Critical bubbles are the ones which, after being created by fluctuations, can grow further. Notice that the surface tension  $\sigma$  is the decisive quantity governing the transition dynamics.

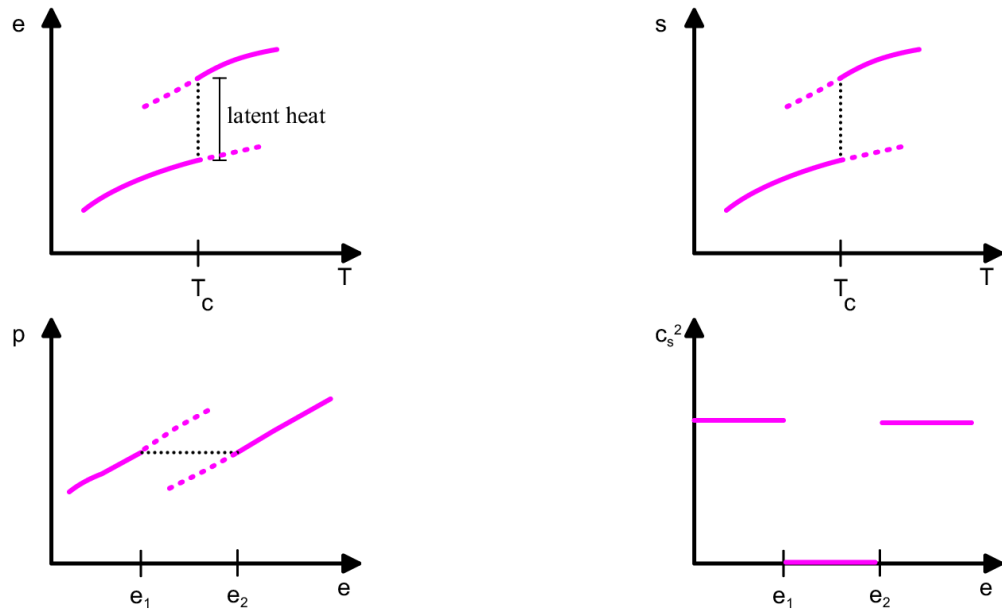


**Fig. 11** Schematic sketch of the thermodynamic state variables for a strong first-order phase transition. Upper row: Energy density  $e$  and entropy density  $s$  as a function of the temperature. Lower row: Pressure  $p$  and sound velocity  $c_s^2 = \partial p / \partial e$  as a function of the energy density.

The probability for forming a critical bubble per time and volume unit is given by

$$w = w_0 \exp \left\{ \frac{-16\pi\sigma^3}{3T(p_1 - p_2)^2} \right\}, \quad (37)$$

where, from dimensional reasons,

$$\sigma = \sigma_0 T_c^3, \quad w_0 = \bar{w}_0 T_c^4 \quad (38)$$

must hold, since the relevant scale is given by  $T_c$ . One usually assumes that  $\sigma_0, \bar{w}_0 \sim \mathcal{O}(1)$ . The calculation of the coefficient  $\bar{w}_0$  is often debated (cf. [33]), but due to the enormously sensitive temperature dependence of the exponent in (37), changes in  $\bar{w}_0$  may be absorbed in a redefinition of  $\sigma_0$  to be discussed below.

Once a critical bubble is created, it grows with velocity  $v = v(T, \dots)$ , where the dots indicate a possible dependence on other state variables or transport coefficients.

Now, we derive an equation for the occupancy of the space with the new phase. Thereby, we must take into account that bubbles created at an earlier instant have grown and that later a reduced volume for bubble nucleation is available. The general growth law  $x = x(t, w, v, R_c, \dots)$  has therefore also memory effects. Several approximations are discussed in [32]. Here we take the so-called Avrami approximation

$$x_2 = 1 - \exp\{-h\}, \quad h = \frac{4\pi}{3} \int_0^t d\tau w(\tau) R(\tau)^3 \left[ \frac{R_c(\tau)}{R(\tau)} + \int_\tau^t d\theta \frac{v(\theta)}{R(\theta)} \right]^3, \quad (39)$$

where  $x_2$  is the volume weight of phase 2.

Fig. 12 displays the outcome of a numerical study of the temperature evolution during confinement. The equations of state (30, 31) are supplemented by the background contribution  $p_{\text{bg}} = d_{\text{bg}} \frac{\pi^2}{90} T^4$ , with  $d_{\text{bg}} = 14.25$ . One observes for vanishing surface tension a quasi-equilibrium transition with negligible supercooling, see the flat section in Fig. 12. Increasing the surface tension parameter  $\sigma_0$  causes a deeper supercooling. Then massive nucleation of many critical bubbles happens. This causes a sudden reheating to  $T_c$ , due to the released latent heat. Then nucleation ceases and the transition proceeds via bubble growth. Further increasing the surface tension smoothes out the transition and leads to a longer duration of the transition era. In the extreme case, hypercooling happens, where the system stays below  $T_c$ .

To summarize the typical scales of the confinement transition in the Big Bang let us mention that the estimates of the transition temperature  $T_c \sim 160$  MeV from lattice QCD yield:

- beginning of the transition at world age  $t_1 \sim 6 \mu\text{sec}$ ,
- end of the transition in case of a near to equilibrium transition with small surface tension  $t_2 \sim 12 \mu\text{sec}$ .

Other characteristic quantities are

- horizon radius  $R_H \sim 10$  km,
- Hubble time  $t_H \sim 10^{-5}$  sec,

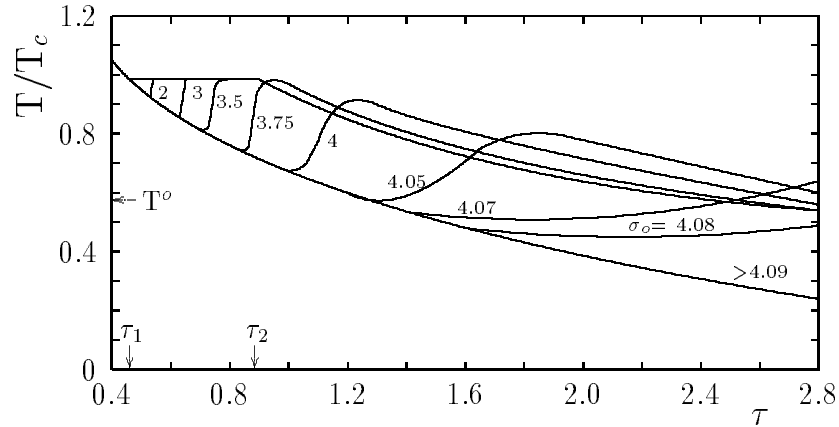


**Fig. 12** The temperature evolution during a first-order phase transition for various values of the surface tension parameter  $\sigma_0$  as a function of the scaled dimensionless time  $\tau = 2CB^{1/2}t$ .  $\tau_1$  and  $\tau_2$  denote the beginning and end of an equilibrium transition;  $T^o$  is the temperature of the maximum nucleation rate (37).

- energy density within the horizon  $M_H$  corresponding to  $\sim 1M_\odot$ ,
- baryon charge within horizon  $N_H^B \sim 10^{50}$ ,
- $e_{CDM} \sim 10^{-8}e_{rad}$  (from a back-extrapolation of estimates of the present cold dark matter energy density).

## 6 Details of the cosmic confinement transition

### 6.1 Small supercooling

Early QCD lattice calculations predicted an astonishingly small surface tension (38) between hadronic and deconfined matter:  $\sigma_0 = 0.0292$  [34], 0.0155 [35], 0.014  $\dots$  0.03 (or 0.44) [36]. As these numbers are valid for pure SU(3) gauge theory, where the deconfinement transition is undoubtedly of first order, one can speculate whether this feature of  $\sigma_0 \ll 1$  is pertinent when the quark degrees of freedom are included. As a consequence, the transition is expected to proceed with small initial supercooling,  $\Delta T/T_c \leq 10^{-3}$ , and follows then the unlabeled flat section in Fig. 12. The temperature is kept constant at  $T_c$  due to the condensation heat released. Therefore, the transition resembles an equilibrium transition since bubbles have time enough to grow and the released latent heat is rapidly distributed uniformly. Entropy production is negligible. The expansion of the scale factor is slightly changed and points to a mini-inflationary era [37], i.e., an expansion faster than  $R \propto \sqrt{t}$ .

An opposite scenario is claimed in [38]. There, within an effective two-phase model with strong first-order phase transition, the possibility of a substantial supercooling is considered and, as a consequence, an exponential growth of the scale factor and

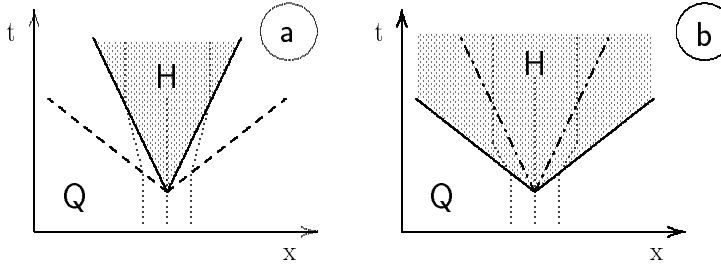


**Fig. 13** Space-time diagram of two types of growing bubbles of hadronic matter (H) in deconfined matter (Q). Left panel: Deflagration bubbles. Right panel: Detonation bubbles. The solid lines are the phase boundaries, while the dashed lines depict shock waves reheating the matter. The dotted lines indicate stream lines of matter. These sketches are strongly stretched in  $x$ -direction so that the light cone is below the dashed lines in (a) and below the solid lines in (b).

a huge entropy increase are advocated. The entropy increase dilutes the baryon-to-photon ratio. For instance, a pre-fabricated ratio  $n_B/n_\gamma \sim \mathcal{O}(1)$  prior to the transition can be diluted to the needed value of  $10^{-9}$  (prior to nucleosynthesis) if the entropy increase is tuned to  $10^9$ . Scenarios of such a type have been elaborated for inflation and will be discussed in section 8. We consider Fig. 8 and notice the small values of the surface tension from lattice QCD. Then the scenario in [38] seems to be too extreme. In particular, during the rapid expansion of matter in the Little Bang such parameters would cause an extremely deep supercooling, in contrast to the expectation [39].

To conclude this subsection, we mention a series of papers [40], in which the confinement transition is studied within an effective theory, namely the dual Ginzburg-Landau model based on the dual Higgs mechanism by QCD monopole condensation.

## 6.2 Turbulent confinement transition?

There are two types of hydrodynamical solutions for growing bubbles in matter being at rest far enough from the bubble [41], as depicted in Fig. 13: Deflagration bubbles and detonation bubbles. In both types, the bubble growth<sup>f</sup> is accompanied by shock waves. If we have deflagration bubbles, these waves propagate in the deconfined phase. Otherwise, the waves occur in the hadronic phase. As suggested by Fig. 14, there are many intersections of the shock waves during the completion of the confinement transition. The intersections are related to density inhomogeneities which we will discuss below. The density inhomogeneities can represent nuclei for black hole formation visible as Hawking flashes or via gravitational lensing or they can cause clumping of dark matter. However, the shock waves are very weak and speculations on resulting strong turbulences are on less firm grounds.

<sup>f</sup>See also [42] for the bubble dynamics at the end of the cosmological confinement transition.

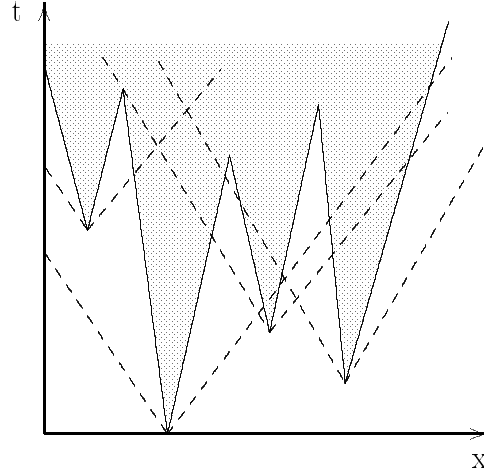


**Fig. 14** Schematic view on the process of filling the space with the confined phase by bubble growth via deflagration. Many intersections of shock waves arise.

### 6.3 Baryon concentration

Let us now discuss a few possible relics of the cosmic confinement transition. On small scales in the order of growing hadron bubbles or vanishing last islands of the quark-gluon plasma (cf. Fig. 15) a baryon concentration arises. According to the scenario of a near-to-equilibrium transition, at the phase boundary also chemical equilibrium is maintained between quarks ( $q$ ) and nucleons ( $N$ ). The reaction  $3q \leftrightarrow N$  is unhindered and, due to detailed balance, causes the balance equation for the baryo-chemical potentials  $3\mu_q = \mu_N$ . Since in the deconfined phase the baryon charge is carried mainly by the light current quarks, while in the confined phase the baryon charge is in the very heavy nucleons (compared to the temperature scale), the relation  $\hat{n}_{QGP}^B \gg \hat{n}_H^B$  emerges from the general expression of the net baryon density  $\hat{n}^B$  (density of baryons minus density of anti-baryons) in ideal gas approximation (cf. (23, 24))

$$\hat{n}^B \approx \begin{cases} \frac{1}{3} N_f T^3 \left(\frac{\mu_q}{T}\right) \left[1 + \frac{1}{\pi^2} \left(\frac{\mu_q}{T}\right)^2\right] = \hat{n}_{QGP}^B, \\ \frac{1}{\sqrt{2\pi^3}} d_N T^3 \left(\frac{m_N}{T}\right)^{3/2} e^{-m_N/T} \frac{\mu_N}{T} = \hat{n}_H^B, \end{cases} \quad (40)$$

where  $N_f$  is the number of excited quark flavors (2 or 3 for  $u, d$  or  $u, d, s$  quarks with negligible masses) and  $d_N = 4$  is the nucleon degeneracy;  $m_N = 939$  MeV denotes the averaged nucleon mass. (40) is for  $\mu_N < m_N$  and in Boltzmann approximation. Due to the exponential suppression factor in (40), the ratio  $\hat{n}_{QGP}^B/\hat{n}_H^B$  at  $T \ll 200$  MeV becomes very large. In fact, the baryon charge is concentrated in the last islands of deconfined matter, as visualized in Fig. 15.

This baryon concentration may cause two interesting effects intensively debated during the last decade: either the quark islands stabilize themselves and survive as quark nugget relics or they convert into isothermal baryon density fluctuations.

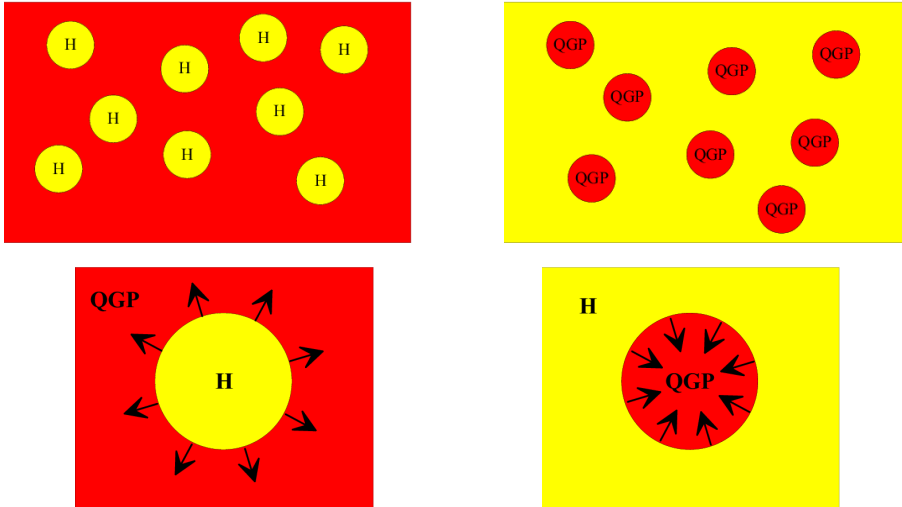


**Fig. 15** Left column: Growing bubbles of hadronic matter immersed in quark-gluon plasma. Right column: Shrinking islands of quark-plasma immersed in hadronic matter. For  $T \ll 200$  MeV, the baryon charge is accumulated in the quark islands.

We will discuss the former effect in the next subsection. The latter effect can affect the primordial nucleosynthesis if it survives up to then. A necessary condition is  $l \sim 1 \text{ m}|_{T=100 \text{ MeV}}$ , where  $l$  is the comoving scale characterizing the mean distance of the inhomogeneities, which is determined by the nucleation process via  $l \sim 0.8(T_c/100 \text{ MeV}) d_{\text{nuc}}$  [43] with

$$d_{\text{nuc}} \approx 13 \left( \frac{145 \text{ MeV}}{B^{1/4}} \right)^2 \left( \frac{4B}{L} \right) \left( \frac{\sigma}{0.035 B^{3/4}} \right)^{3/2} \text{ cm}; \quad (41)$$

$L$  is the latent heat in the bag model (30, 31), cf. left upper panel in Fig. 11.

In confined matter the neutrons can rapidly diffuse thus causing an inhomogeneous neutron-to-proton ratio. Recent re-analyses [43, 44] let this scenario appear less probable: the low surface tension, discussed in subsection 6.1, gives rise to a typical scale  $l \sim 1 \text{ cm}$  and the detailed study of the nucleosynthesis shows no deviations from the homogeneous standard scenario.

It should be mentioned, however, that the estimates quoted above rely on the homogeneous nucleation theory. Nucleation by impurities is more efficient and, as shown in [43], can indeed render the inhomogeneity scale to  $l \sim 1 \text{ m}$ , supposed there are pre-fabricated fluctuations or impurities on an appropriate scale, such as vortices, domain walls, magnetic monopoles, cosmic strings, or relic fluctuations from the electroweak transition. The required scale of  $l \sim 1 \text{ m}$  corresponds just to the red-shifted horizon scale at the electroweak transition (see below). In [45] it is pointed out that temperature fluctuations, compatible with the COBE measurements, can give rise to an inhomogeneous nucleation with interesting consequences.

Another idea is that a sufficiently large baryon concentration can survive up to now in form of quark nuggets being thus candidates for dark matter. For a recent

discussion cf. [46]. The quark nuggets must have baryon charges of  $N^B \sim 10^{40 \dots 45}$  because otherwise the baryon contrast would have diffused away.

#### 6.4 Strange matter

Strangeness may play a particular role in the cosmic evolution. While nowadays the hadrons are mainly nucleons with the valence quark structure  $p = (uud)$ ,  $n = (ddu)$ , just after confinement also pions and kaons were present. Kaons carry strangeness, e.g.  $K^+ = (u\bar{s})$ , but once the universe cools below 100 MeV they rapidly decay, and the strange particles disappear from the world. They can be afterwards newly created for a short while by strong interaction of high-energy cosmic rays with matter and in the laboratory. But the earlier universe was quite strange. Due to the long expansion and cooling time scales in comparison with the time scale of the weak interaction, there was chemical equilibrium according to the reactions changing strangeness

$$d \leftrightarrow u + e^- + \bar{\nu}_e, \quad s \leftrightarrow u + e^- + \bar{\nu}_e. \quad (42)$$

This results in the balance equations

$$\mu_d = \mu_u + \mu_{e^-} - \mu_{\nu_e}, \quad \mu_s = \mu_u + \mu_{e^-} - \mu_{\nu_e}, \quad (43)$$

from which  $\mu_s = \mu_d$  follows, or  $n_s \approx n_d$ . Thus, a substantial part of the quarks were strange ones (for a more detailed consideration including charge neutrality cf. [32]). As pointed in [47, 48], within the bag model the strange quarks can stabilize the quark matter. This idea is re-analyzed with increasing sophistication [49] and there seems to be a region in the parameter space still leaving the possibility of stable strange quark nuggets. These represent candidates for dark matter.

The dedicated experiments with heavy-ion collisions, however, did not show positive signals of strangelets [50]. This constrains the parameter space further and makes the strangelet idea less probable. It should be stressed, however, that in heavy-ion collisions the time scales are much shorter and the conditions for creating strangelets may be less favorable.

#### 6.5 Effects of vanishing sound velocity

As seen in Fig. 11 the sound velocity vanishes in first-order phase transitions in the mixed phase. This observation has an important effect on the evolution of fluctuations: the restoring pressure gradient of density-enhanced regions vanishes, and these regions can collapse in free fall.

##### 6.5.1 Intermediate scales

On intermediate scales,  $l \ll \lambda \ll R_H$ , the fate of the fluctuations is followed by the cosmological perturbation formalism [51]. In particular, as pointed out in [51], kinetically decoupled cold dark matter can be trapped in gravitational wells. Candidates for such dark matter are WIMPzillas<sup>§</sup> ( $M > 10^6$  GeV), primordial black holes ( $10^{-18} M_\odot \ll M < M_\odot$ ), and axions ( $M \sim 10^{-5}$  eV) which can be accumulated

<sup>§</sup>This nickname refers to the notion of Weakly Interacting Massive Particles, see [52].

to lumps with mass of  $M \sim 10^{-(10 \dots 20)} M_\odot$ . Also primordial gravitational waves are modified, however, on scales today not accessible via pulsar timing. Afterwards, the neutrino diffusion is efficient enough to damp away the created density fluctuations till nucleosynthesis, unless the decoupled matter lumps.

### 6.5.2 Horizon scales

As pointed out in [53], on large scales,  $\lambda \sim R_H$ , already previous causally non-connected weak fluctuations on super-horizon scales can, after entry into the horizon, collapse to black holes with  $M \sim 1M_\odot$  due to  $c_s^2 = 0$  during confinement (cf. [51] for a further discussion). Such a mechanism can produce MACHOs<sup>h</sup> visible by gravitational lensing.

### 6.5.3 Vanishing sound velocity during confinement?

Since both effects are related to the vanishing of the sound velocity, one has to analyze whether this may really happen. In the case of a strong crossover, instead of first-order phase transition, the sound velocity decreases but does not vanish completely. As shown in [51] under such circumstances the resulting gravitational wells are too weak to substantially capture dark matter.

One has also to mention that  $c_s^2 = 0$  holds only for  $p = const$  in the phase mixture region when all chemical potentials  $\mu_\alpha$  vanish or only one independent chemical potential occurs, i.e.,  $\alpha = 1$ . In cosmic matter there are numerous potentials, such as  $\mu_e, \mu_\mu, \mu_{\nu's}, \mu_u, \mu_d, \mu_p, \mu_n$ .

Imposing  $\beta$  equilibrium, according to (42) and  $n \leftrightarrow p + e^- \bar{\nu}_e$ , and local electric charge neutrality, at least one of the chemical potentials changes discontinuously in the case of a naively constructed phase transition. Instead, as stressed in [55], constructing the phase equilibrium with the averaged charge neutrality  $n_{had} + n_{QGP} = 0$  results (cf. Fig. 16) in  $p \neq const$  in the mixed state, and therefore the sound velocity does not strictly vanish. The effect of the various chemical potential may be small if  $\mu_\alpha \ll T$  and the sound velocity at least substantially drops in the mixed state.

Otherwise one should notice that upon approaching the confinement temperature the sound velocity in the deconfined state itself already drops (cf. Fig. 17). This is usually related to a softening of the equation of state. In [56] evidences of such a softening is extracted from data of heavy-ion collisions at AGS energies. It is matter of debate whether this is an indication of deconfinement effects at such comparatively low beam energies of  $10 \dots 15$  A·GeV.

Moreover, the annihilation process of certain particle species is also related to a decrease of the sound velocity, cf. [51]. This turns out to be a marginal effect. To look into details let us consider the era when the muons disappear. At  $T \gg m_\mu$  and at  $T \ll m_\mu$  the degeneracies are  $d_{eff} = 14.25$  and  $10.75$ , respectively. By evaluating numerically the statistical integral (25), one gets the pressure as displayed in Fig. 18. Indeed, there is a small change of the scaled total pressure at  $T/m_\mu \sim 0.4$ . At  $T/m_\mu < 0.2$ , the muons can be neglected and at  $T/m_\mu > 1$  the radiation approximation,  $p_\mu = \frac{d_\mu \pi^2}{90} T^4$  with  $d_\mu = 4$ , is sufficient.

<sup>h</sup> MACHO is an acronym for Massive Compact Halo Objects, see [54].

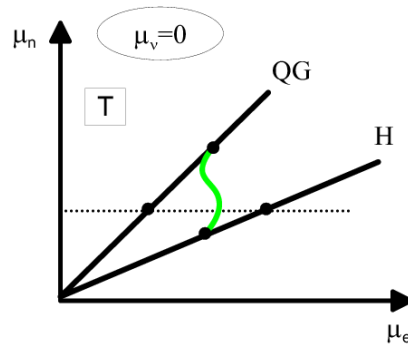


**Fig. 16** Constructing the phase transition in presence of a some chemical potentials. Imposing charge neutrality yields the two curves labeled by QG and H for deconfined and confined matter, respectively. Pressure equality at fixed temperature and at equal neutron-baryon chemical potential  $\mu_n$  (indicated by the dotted line) is connected with a jump of the electron chemical potential  $\mu_e$ . Instead, averaged charge neutrality results in the gray S-shaped line. On this line, the pressures of both phases are equal but they change when moving along this line.

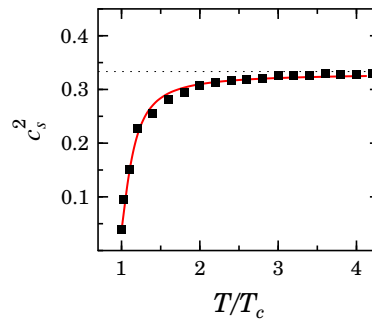


**Fig. 17** The sound velocity of gluon matter as a function of temperature. Symbols depict the results of lattice QCD data from the group Bielefeld and the curve results from the quasi-particle model [24].

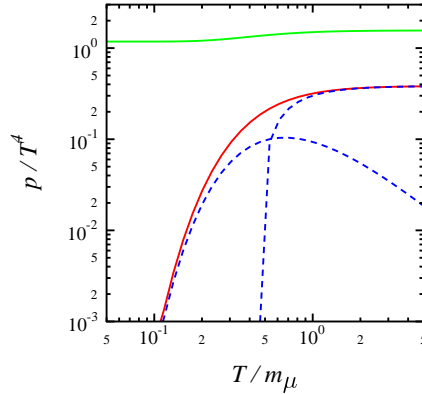


**Fig. 18** The scaled pressure as a function of the temperature of the muons (lower solid line: exact evaluation of the statistical integral (24), dashed lines: using the first two terms of the high and low temperature expansion). Upper gray curve: total pressure taking into account the background of electrons, photons, and three neutrino species.

Solving the evolution equations (14, 15) results in the temperature history as displayed in the left panel of Fig. 19. There is a very moderate change of the cooling due to muon annihilation. Only when incorrectly approximating the muon pressure by the first two terms in the high-temperature expansions one gets a more pronounced effect which looks like a phase transition (see right panel of Fig. 19).

Thus the effect of particle annihilation is weak and unlikely to cause a reheating or a substantial softening of the equation of state. This can also be seen from the measure  $3p/e$  which drops from 1 to 0.95 during muon annihilation and rises to 1 afterwards. Therefore, particle annihilation can hardly cause strong effects, as mentioned in [51].

### 6.6 Interim resume

The confinement transition is quite interesting, but the cosmic evolution is already slow compared with the strong interaction time scale, and probably the most severe effects are washed out. Quasi-equilibrium means memory loss. In addition some details are poorly known, such as the correct order of the transition and the surface tension (if any). Therefore, one might argue that earlier stages with more rapid evolution are out of equilibrium and do not leave such fragile imprints.

## 7 Electroweak symmetry breaking

In the electroweak standard model à la Glashow-Salam-Weinberg the Higgs field is responsible for the dynamical mass generation via spontaneous symmetry breaking. At sufficiently high temperatures,  $T > 100$  GeV, the expectation value of the Higgs field is zero, i.e., the symmetry is restored and particles are massless. At  $T < 100$  GeV

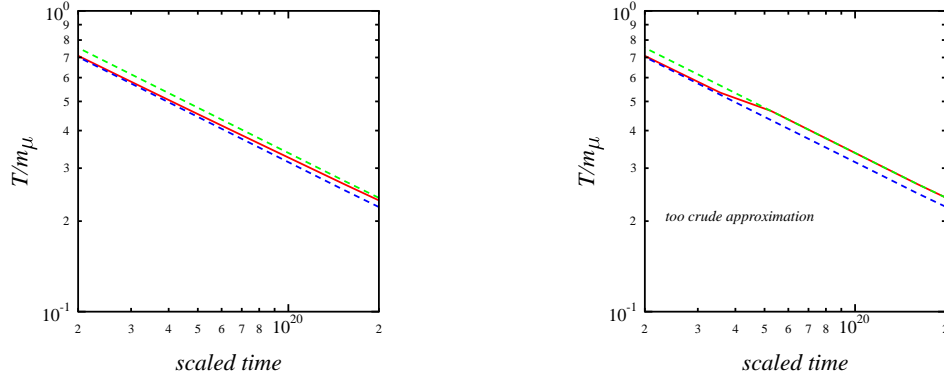


**Fig. 19** The evolution of the temperature as a function of the scaled time. Lower dashed line: only the background, upper dashed line: background plus massless muons, solid line: background plus muon contribution. The left panel uses the correct evaluation of the pressure, while the right panel employs only the expansion described in text.

the symmetry becomes broken because  $\langle \text{Higgs} \rangle \neq 0$  and particle masses become finite. For Higgs masses  $m_H < 75$  GeV, the symmetry breaking appears as weak first-order phase transition, while for the more likely case of  $m_H > 75$  GeV a phase transition of second order happens [57, 58]. Indeed, approaching  $m_H \rightarrow 75$  GeV, the surface tension drops dramatically [58]. In view of the experience with the confinement transition, one may not expect drastic effects from this transition.

However, there is an important issue, outside the scope of the present work, related to non-perturbative effects of solitary field configurations called sphalerons: baryon and lepton numbers are not conserved. Therefore, at the electroweak transition the baryon and lepton excess of the universe might be generated. Since a final consistent picture does not seem to be elaborated yet, we refer to some recent surveys on this topic including also energies of the GUT scale, see [59].

## 8 Inflation

Equation (16) shows that at  $p < -\frac{1}{3}e$  the expansion of the universe becomes accelerated. In particular, if the vacuum energy density dominates, i.e.  $e^{\text{vac}} \gg e_\alpha$  and  $e = e^{\text{vac}} = -p^{\text{vac}} \approx \text{const}$  then  $R \propto e^{C\sqrt{e^{\text{vac}}t}}$ . A series of problems in modern cosmology is solved by inflation if the scale factor  $R$  grows in the inflationary period by a factor of about  $10^{30}$ . These standard problems, like horizon, flatness, homogeneity, age, and monopole problems, are summarized in many surveys, see [16].

Inflation can be realized within a model with a dominating spatially homogeneous scalar field which, via a potential  $V(\phi)$ , is self-interacting. The corresponding equation of state can be deduced from

$$e = +V(\phi, T) + \frac{1}{2}\dot{\phi}^2, \quad (44)$$

$$p = -V(\phi, T) + \frac{1}{2}\dot{\phi}^2 \quad (45)$$

(quantum corrections cause a temperature dependence of the effective potential). For a sufficiently slow evolution, the kinetic term can be neglected and the coherent field mimics a perfect vacuum. Inflation is expected to happen on the GUT scale of  $T \sim 10^{16}$  GeV and provides, via adiabatic Gaussian fluctuations, the seed for later structure formation. The various inflationary scenarios differ essentially only in the choice of the potential. To recall a few scenarios (cf. [60]):

- old inflation: decay of a metastable (“wrong”) vacuum caused by a potential with two local minima corresponding to a phase transition of first order,
- new inflation: a potential which is very flat around  $\phi_i = 0$ , where  $\phi_i$  is the initial state, and which has a minimum at  $\phi_R > 0$ ,
- chaotic inflation: a simple U-shaped potential and  $\phi_i \gg 0$  evolving to  $\phi_R = 0$ ,
- hybrid inflation: two coupled scalar fields with  $\varphi \gg \phi$ , and  $\phi$  evolves in the slow rolling down potential of new inflation.

We do not consider here scenarios beyond Einstein’s theory or involving supersymmetry or string theory.

### 8.1 Viscous inflation

The original version of the old inflationary scenario [61] assumed a supercooling by 30 orders of magnitude to achieve the stretching of  $R$  by 30 order of magnitudes. Then, of course, the exponential grow of the space prevents a graceful exit to a homogeneous state after reheating. However, there are also phenomenological ansätze which realize successful inflation without such tremendous supercooling. For instance, in viscous inflation [62] a suitably tuned volume viscosity can compensate the cooling, moreover, due to the replacement of the pure thermodynamic pressure  $p$  by  $p - 3\frac{\dot{R}}{R}\hat{\xi}$  (see (6)), the space expansion can accelerate for suitable values of  $\hat{\xi}$ . Then there happens a tremendous entropy production. To be specific, an increase of the comoving entropy,  $sR^3$ , by a factor  $10^{90}$  is sufficient to solve most of the standard problems. The key here is entropy production, which spoils the comoving entropy conservation and such an information link of very early and late stages of the universe.

### 8.2 Tepid inflation

Another way of entropy production is a phase transition with supercooling. Let us consider as an example an isothermal phase transition at  $T = \text{const}$ , as visualized in the left panel of Fig. 20. The state of matter changes as indicated in the middle panel by the solid vertical arrow, i.e., there is a transition where the new phase (2) has larger pressure than the old phase (1). This causes a compression of the regions filled with the old phase. Taking into account the averaging prescription for the energy density during the phase transition

$$e = e_1x + e_2(1 - x) \quad (46)$$

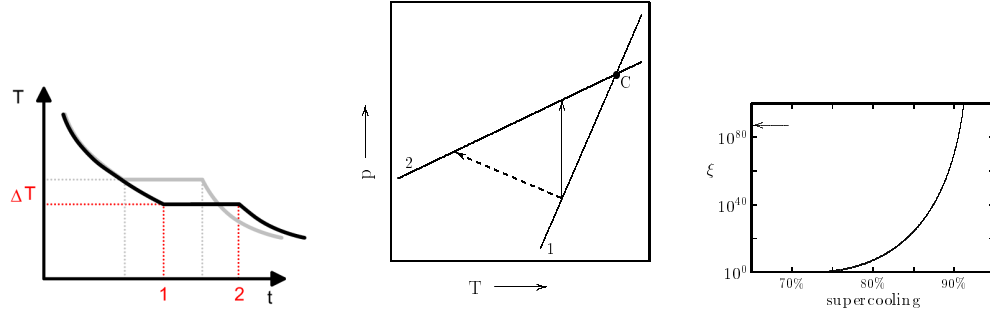


**Fig. 20** Left panel: Isothermal phase transition with supercooling  $\Delta T$  (heavy solid curve). Middle panel: Sketch of the equation of state near the equilibrium point “C”. Right panel: Entropy increase as a function of supercooling.

and analog equations for the pressure and the entropy density, the entropy increase for the perfect 2-phase fluid is found from (7) as

$$(sR^3) = R^3 \left\{ \frac{2}{T_1 + T_2} (p_1 - p_2) \dot{x} + (T_1 - T_2) \left[ \dot{\Delta} + 3 \frac{\dot{R}}{R} \Delta \right] \right\}, \quad (47)$$

$$\Delta = xs_1 - (1-x)s_2,$$

instead of  $(sR^3) = 0$  for the ideal 1-component fluid. To quantify the entropy production let us define an entropy increase factor by  $\xi = \frac{sR^3}{s_i R_i^3}$ . This factor is displayed in the right panel of Fig. 20 as a function of the supercooling. One observes that moderate supercooling in the order of 90 - 95% is sufficient for successful inflation.

In [63] we have discussed a more dynamical model with a phase transition and an ansatz for the relaxation time approximation for  $x_2(t)$ . We find a sufficient tepid inflation. Now we consider the nucleation theory, presented in section 5, and study the evolution of the scale factor and the entropy increase. The results of a numerical integration of the evolution equations (14, 15, 37, 39) are presented in Fig. 21. There are two regimes:

- (i) a too small surface tension parameter  $\sigma_0$  causes a too small supercooling and insufficient inflation, while
- (ii) a too large value of  $\sigma_0$  repeats the graceful exit problem of old inflation, i.e. the space is exponentially growing, and the growth of bubbles is too slow to fill the space, as visualized in Fig. 22.

However there is a small corridor in parameter space where we find power law inflation with  $R \sim t^\alpha$ ,  $\alpha > 1$ , resembling the extended inflation in Brans-Dicke theory. Numerically it is difficult to follow a successful inflationary evolution due to the needed fine tuning of  $\sigma_0$  and the accuracy of the integration procedure with respect to the large number problems. Therefore, it is hard to make statements on the emerging fluctuation spectrum.

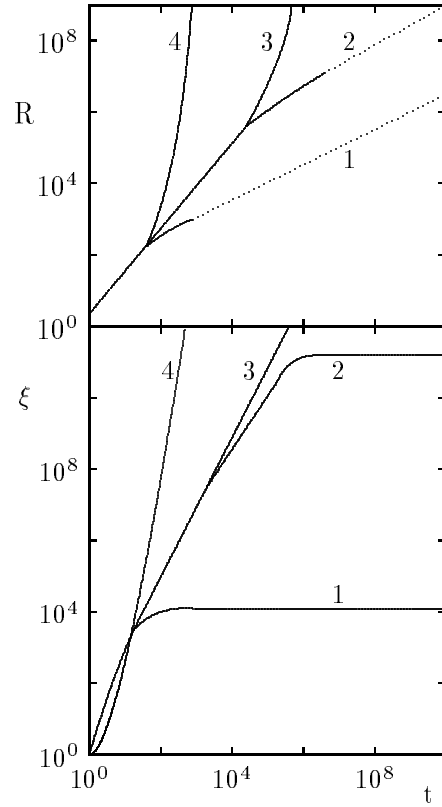


**Fig. 21** Evolution of the scale factor (upper panel) and the entropy increase factor (lower panel) as a function of time. The dotted sections in the upper panel correspond to the flat sections in the lower panel and indicate that the old phase disappeared. Curves labeled by 1, 2, 3, 4 correspond to  $\sigma_0 = 2.064, 2.06499, 2.065, 2.066$ , respectively. For more details, like the parameterization of the equation of state, consult [32, 64].

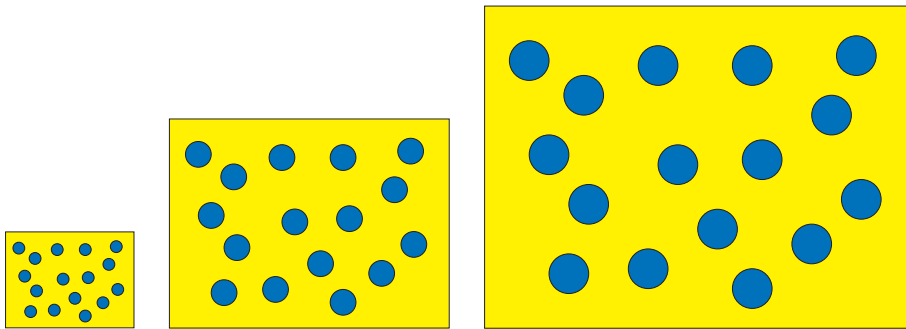


**Fig. 22** Visualization of the graceful exit problem: the space expands too rapidly and the growing bubbles fail to percolate since nucleation is, due to large supercooling, too rare to fill the space.

## 9 Summary

We should be aware that the evolution of the universe is accompanied by a permanent change of the states of matter, which can be in some interesting cases be considered as phase transitions. There is a change of certain order parameters, like a hypothetical scalar field  $\phi$  on the GUT scale, the Higgs field on the electroweak scale, the chiral condensate on the QCD scale, or even now the quintessence. This causes partially drastic changes of matter like the transition from freely roaming quarks and gluons to hadrons, or the binding of nucleons into light nuclei during nucleosynthesis, or simply the annihilation of particles like  $e^+e^- \rightarrow 2\gamma$ . These changes induce also changes of the expansion dynamics of the universe, most drastic during inflation, e.g.. Furthermore in the transition from a radiation dominated universe to a matter dominated one, the time-evolution of the scale factor  $R(t)$  changes from  $R \propto t^{1/2}$  to  $R(t) \propto t^{2/3}$ . Some uncertainty is introduced by the evidence recently found of a dominating vacuum energy density, the quintessence, because its back-extrapolation needs more definite knowledge on its nature.

Assuming that in early stages quintessence is not dominating the energy density, we considered in some detail the confinement transition in the Big Bang and, very briefly, contrasted it to the Little Bang, presently investigated in heavy-ion collision experiments. In the Little Bang one observes direct electromagnetic radiation like real photons and virtual photons via  $\gamma^* \rightarrow e^+e^-$ . This points to temperature scales of 170 MeV and larger, i.e., above the deconfinement transition. In contrast to this, there do not seem to be specific definite relics from the confinement era of the Big Bang, apart the protons and neutrons created in hadrosynthesis. We summarized possible relics, whose existence is hypothetical and the predictions of which are sometimes related to poorly known details of the confinement dynamics.

Whereas the results of the nucleosynthesis processes specifically depend on the interplay of neutrino decoupling, neutron life time, and cosmic cooling rate, the hadrosynthesis at confinement seems to be rather unspecific. Nucleons emerge as other hadrons do as well, but the unstable hadrons decay shortly after confinement and the proton-to-neutron ratio is determined by  $\beta$  equilibrium. Hence, hadrosynthesis does not cause a specific hadron composition due to the cosmic evolution since chemical equilibrium means memory loss.

Strictly speaking, the success of the primordial nucleosynthesis makes us strongly believe in a maximum temperature of  $T_R > 1$  MeV, while the prediction of a flat universe and of an appropriate fluctuation spectrum for structure formation by inflationary scenarios makes us believe in  $T_R > 10^{15}$  GeV. Within these scales, a consistent picture of the evolution of the universe seems to emerge, but it leaves a consistent treatment of the “initial state” and the reheating (or, better, “pre-heating”) to  $T_R$  as the most challenging problem probably to be solved within quantum gravity.

Acknowledgments: K. Gallmeister is grateful for preparing the figures. I thank F.W. Hehl and A. Gross for carefully reading the manuscript. Some of the presented material is an up-grade of [32]. The author thanks his colleagues for the fruitful collaboration. The work is supported in part by BMBF grant 06DR829/1.

## References

- [1] A.O. Barvinsky, A.Yu. Kamenshchik, C. Kiefer, *Mod. Phys. Lett.* **A 14** (1999) 1083
- [2] H. Schulz, B. Kämpfer, H.W. Barz, G. Röpke, J. Bondorf, *Phys. Lett.* **B 147** (1984) 17
- [3] V. Serfling et al. (ALADIN Collaboration), *Phys. Rev. Lett.* **80** (1998) 3928  
J. Pochodzalla et al. (ALADIN Collaboration), *Phys. Rev. Lett.* **75** (1995) 1040
- [4] D. Boyanovsky et al., astro-ph/9707267, hep-ph/9903534, hep-ph/9911521
- [5] <http://press.web.cern.ch/Press/Releases00/PR01.00EQuarkGluonMatter.html>
- [6] <http://oposite.stsci.edu/pubinfo/PR/96/01.html>
- [7] M. Hentschel et al., *Z. Phys.* **C 75** (1997) 333
- [8] K. Gallmeister, B. Kämpfer, O.P. Pavlenko, *Eur. Phys. J.* **C 8** (1999) 473  
B. Kämpfer, O.P. Pavlenko, *Phys. Atom. Nucl.* **58** (1995) 2144
- [9] S. Perlmutter, M.S. Turner, M. White, *Phys. Rev. Lett.* **83** (1999) 670  
S. Perlmutter et al., astro-ph/9812133
- [10] H. Ziaeeepour, astro-ph/0002400  
S. Perlmutter et al., *Ap. J.* **517** (1999) 565
- [11] L. Bergström, hep-ph/0002126  
A.D. Dolgov, hep-ph/9910532
- [12] W.L. Freeman, astro-ph/9909134  
B. Chaboyer, *Phys. Rep.* **307** (1998) 23
- [13] I. Zlatev, P.J. Steinhardt, *Phys. Lett.* **B 459** (1999) 570  
P.J. Steinhardt, L. Wang, I. Zlatev, *Phys. Rev.* **D 59** (1999) 123504
- [14] P. Brax, J. Martin, *Phys. Rev.* **D 61** (2000) 103502  
F. Ferrota, C. Baccigalupi, S. Matarrese, *Phys. Rev.* **D 61** (2000) 023507  
T. Chiba, *Phys. Rev.* **D 60** (1999) 083508  
I. Zlatev, L.M. Wang, P.J. Steinhardt, *Phys. Rev. Lett.* **82** (1999) 896  
S.M. Carroll, *Phys. Rev. Lett.* **81** (1999) 3067  
R.R. Caldwell, R. Dave, P.J. Steinhard, *Phys. Rev.* **80** (1998) 1582
- [15] S. Weinberg, astro-ph/0002387  
E. Witten, hep-ph/0002297  
S. Weinberg, *Rev. Mod. Phys.* **61** (1989) 1  
V. Sahni, A. Starobinsky, astro-ph/9904398
- [16] P. Coles, F. Lucchin, *Cosmology*, John Wiley & Sons, Chichester New York Brisbane Toronto Singapore 1995
- [17] [http://nssdca.gsfc.nasa.gov/anon\\_dir/cobe/images/dmr/cmb\\_fluctuations\\_big.gif](http://nssdca.gsfc.nasa.gov/anon_dir/cobe/images/dmr/cmb_fluctuations_big.gif)  
<http://space.gsfc.nasa.gov/astro/cobe>
- [18] W.A. Hiscock, L. Lindblom, *Ann. Phys.* **151** (1983) 466  
W. Israel, J.M. Steward, *Ann. Phys.* **118** (1979) 341
- [19] K. Geiger, *Phys. Rep.* **258** (1995) 237  
X.N. Wang, *Phys. Rep.* **280** (1997) 287
- [20] J.D. Bjorken, *Phys. Rev.* **D 27** (1983) 140
- [21] K. Gallmeister, B. Kämpfer, O.P. Pavlenko, *Phys. Lett.* **B 473** (2000) 20
- [22] B. Kämpfer, O.P. Pavlenko, *Phys. Lett.* **B 391** (1997) 185
- [23] T. Muta, *Foundations of quantum chromodynamics*, World Scientific, Singapore New Jersey London Hong Kong 1998  
D. Bailin, A. Love, *Introduction to gauge field theory*, Institute of physics publishing, Bristol Philadelphia 1994
- [24] A. Peshier, B. Kämpfer, G. Soff, *Phys. Rev.* **C 61** (2000) 045202  
A. Peshier, B. Kämpfer, O.P. Pavlenko, G. Soff, *Phys. Rev.* **D 54** (1996) 2399
- [25] A. Peikert, F. Karsch, E. Laermann, B. Sturm, *Nucl. Phys. Proc. Suppl.* **73** (1999) 468
- [26] K. Rajagopal, *Nucl. Phys.* **A 661** (1999) 150c
- [27] P. Braun-Munzinger, I. Heppe, J. Stachel, *Phys. Lett.* **B 465** (1999) 15
- [28] H. Heiselberg, V. Pandharipande, astro-ph/0003276  
H. Heiselberg, M. Hjorth-Jensen, *Phys. Rep.* **328** (2000) 237  
A. Akmal, V.R. Pandharipande, D.G. Ravenhall, *Phys. Rev.* **C 58** (1998) 1804  
Abd-Alla, S.A. Hager, *Phys. Rev.* **C 61** (2000) 044313

- H. Shen, H. Toki, K. Oyamatsu, K. Sumiyoshi, Nucl. Phys. **A 637** (1998) 435  
 R. Rapp, J. Wambach, Phys. Rev. **C 53** (1996) 3057  
 K.C. Chase, A.Z. Mekjian, Phys. Rev. Lett. **75** (1995) 4732
- [29] L.V. Bravina et al., Phys. Rev. **C 60** (1999) 024904  
 E.L. Bratkovskaya, et al., nucl-th/0001008  
 W. Cassing, E.L. Bratkovskaya, Phys. Rep. **30** (1999) 65
- [30] <http://www.gsi.de/EOS2000/discussion.php3>  
 [31] J.P. Blaizot, J.Y. Ollitrault, Phys. Lett. **B 191** (1987) 21, Phys. Rev. **D 36** (1987) 916  
 [32] B. Kämpfer, B. Lukács, G. Paál, *Cosmic phase transitions*, Teubner-Verlag, Stuttgart Leipzig 1994
- [33] L.P. Csernai, J.I. Kapusta, Phys. Rev. Lett. **69** (1992) 737, Phys. Rev. **D 46** (1992) 1379
- [34] Y. Iwasaki, K. Kanya, L. Kärkkäinen, K. Rummukainen, T. Yoshié, Phys. Rev. **D 49** (1994) 3540
- [35] B. Beinlich, F. Karsch, A. Peikert, Phys. Lett. **B 390** (1997) 268  
 [36] A. Papa, Phys. Lett. **B 420** (1998) 91  
 [37] L.L. Jenkowsky, B. Kämpfer, V.M. Sysoev, Z. Phys. **C 48** (1990) 147,  
 B. Kämpfer, Astron. Nachr. **307** (1986) 231, **309** (1988) 19, 347, **310** (1989) 203  
 V.G. Boyko et al., Anstron. Nachr. **311** (1990) 265  
 A. Bonometteo, O. Pantano, Phys. Rep. **228** (1993) 175
- [38] N. Borhini, W.N. Cottingham, R. Vinh Mau, hep-ph/0001284  
 [39] E.E. Zabrodin et al., Phys. Lett. **B 423** (1998) 373  
 [40] H. Suganuma et al., hep-ph/9608335, Prog. Theor. Phys. Suppl. **120** (1995) 57  
 H. Ichie, H. Suganuma, H. Toki, Phys. Rev. **D 52** (1995) 2944  
 H. Monden, H. Suganuma, H. Ichie, H. Toki, Phys. Rev. **C 57** (1998) 2564
- [41] J. Ignatius et al., Phys. Rev. **D 49** (1994) 3854, **D 50** (1994) 3738  
 M. Gyulassy et al., Nucl. Phys. **B 237** (1984) 477
- [42] L. Rezzolla, Phys. Rev. **D 54** (1996) 6072  
 L. Rezzolla, J.C. Miller, Phys. Rev. **D 53** (1996) 5411  
 L. Rezzolla, J.C. Miller, O. Pantano, Phys. Rev. **D 52** (1995) 3202
- [43] M.B. Christiansen, J. Madsen, Phys. Rev. **D 53** (1996) 5446  
 [44] I.S. Suh, G.J. Mathews, Phys. Rev. **58** (1998) 123002  
 G.M. Fuller, G.J. Mathews, C.R. Alcock, Phys. Rev. **D 37** (1988) 1380  
 K. Sumiyoshi, T. Kajino, C.R. Alcock, G.J. Mathews, Phys. Rev. **D 42** (1990) 3963  
 C.R. Alcock et al., Phys. Rev. Lett. **64** (1990) 2607  
 B.S. Meyer, C.R. Alcock, G.J. Mathews, G.M. Fuller, Phys. Rev. **D 43** (1991) 1079
- [45] J. Ignatius, D.J. Schwarz, hep-ph/0004259  
 [46] A. Bhattacharyya et al., Phys. Rev. **D 61** (2000) 083509  
 H.I. Kim, B.H. Lee, C.H. Lee, astro-ph/9901286
- [47] E. Farhi, R.L. Jaffe, Phys. Rev. **D30** (1994) 2379  
 [48] E. Witten, Phys. Rev. **D 30** (1984) 272  
 [49] C. Alcock, A. Olinto, Phys. Rev. **D 39** (1989) 1233  
 J. Schaffner-Bielich, Nucl. Phys. **A 639** (1998) 443c  
 J. Schaffner-Bielich, C. Greiner, A. Diener, H. Stöcker, Phys. Rev. **C 55** (1997) 3038  
 J. Madsen, in *Hadrons in dense matter and hadrosynthesis*, (Eds.) J. Cleymans, H.B. Geyer, F.G. Scholtz, Lecture Notes in Physics, Springer-Verlag, Berlin Heidelberg New York 1999, p. 162
- [50] G. van Buren et al. (E864 Collaboration), J. Phys. **G 25** (1999) 411  
 G. Appelquist et al. (NA52 Collaboration), Phys. Rev. Lett. **76** (1996) 3907
- [51] D.J. Schwarz, C. Schmid, P. Widerin, astro-ph/9903319  
 C. Schmid, D.J. Schwarz, P. Widerin, Phys. Rev. **D 59** (1999) 043517  
 D.J. Schwarz, Nucl. Phys. **A 642** (1998) 336c  
 D.J. Schwarz, Mod. Phys. Lett. **A 13** (1998) 2771  
 C. Schmid, D.J. Schwarz, P. Widerin, Phys. Rev. Lett. **78** (1997) 791
- [52] D.J.H. Chung, E.W. Kolb, A. Riotto, Phys. Rev. **D 59** (1999) 023501  
 H. Ziaepour, astro-ph/0005299

- 
- [53] K. Jedamzik, J.C Niemeyer, Phys. Rev. **D 59** (1999) 124014  
J.C. Niemeyer, K. Jedamzik, Phys. Rev. **D 59** (1999) 124013  
P. Widerin, C. Schmid, astro-ph/9808142  
K. Jedamzik, Phys. Rep. **307** (1998) 155, Phys. Rev. **D 55** (1997) 5871
- [54] K. Ioka, T. Tanaka, T. Nakamura, Phys. Rev. **D 60** (1999) 083512  
C. Alcock et al. (MACHO collaboration), astro-ph/0001272
- [55] N.K. Glendenning, Phys. Rev. **D 46** (1992) 1274
- [56] P. Danielwicz et al., Phys. Rev. Lett. **81** (1998) 2438
- [57] K. Kajantie et al., hep-ph/9809435, Phys. Rev. Lett. **77** (1996) 2887
- [58] M. Gürtler, E.M. Ilgenfritz, A. Schiller, Phys. Rev. **D 56** (1997) 3888, Eur. Phys. J. **C 1** (1998) 363
- [59] R. Allahverdi, B.A. Campbell, J. Ellis, hep-ph/0001122  
A. Riotto, M. Trodden, Ann. Rev. Nucl. Part. Sci. **49** (1999) 35  
R. Brandenberger, I. Halperin, A. Zhitnitsky, hep-ph/9903318, hep-ph/9808471  
V.A. Rubakov, M.E. Shaposhnikov, hep-ph/9603208
- [60] R.H. Brandenberger, hep-ph/9910410  
A.H. Guth, astro-ph/0002156
- [61] A.H. Guth, Phys. Rev. **D 23** (1981) 347
- [62] L. Diósi, B. Keszthelyi, B. Lukács, G. Paál, Phys. Lett. **B 159** (1988) 23  
L. Herrera, A. Di Priso, D. Pavón, gr-qc/9912043
- [63] B. Kämpfer, B. Lukács, G. Paál, Phys. Lett. **B 187** (1987) 17
- [64] B. Kämpfer, Astrophys. Sp. Sci. **158** (1989) 35